NANO LETTERS

2009
Vol. 9, No. 2
612-616

Hybrid Tin Oxide Nanowires as Stable and High Capacity Anodes for Li-Ion Batteries

Praveen Meduri,[†] Chandrashekhar Pendyala,[†] Vivekanand Kumar,[†] Gamini U. Sumanasekera,[‡] and Mahendra K. Sunkara*,[†]

Department of Chemical Engineering, Department of Physics, University of Louisville, Louisville, Kentucky 40292

Received September 21, 2008; Revised Manuscript Received December 7, 2008

ABSTRACT

In this report, we present a simple and generic concept involving metal nanoclusters supported on metal oxide nanowires as stable and high capacity anode materials for Li-ion batteries. Specifically, SnO_2 nanowires covered with Sn nanoclusters exhibited an exceptional capacity of >800 mAhg^{-1} over hundred cycles with a low capacity fading of less than 1% per cycle. Post lithiation analyses after 100 cycles show little morphological degradation of the hybrid nanowires. The observed, enhanced stability with high capacity retention is explained with the following: (a) the spacing between Sn nanoclusters on SnO_2 nanowires allowed the volume expansion during Li alloying and dealloying; (b) high available surface area of Sn nanoclusters for Li alloying and dealloying; and (c) the presence of Sn nanoclusters on SnO_2 allowed reversible reaction between Sn and Li_2O to produce both Sn and SnO phases.

One-dimensional, nanowire (NW)-based materials are promising candidates for lithium-ion (Li-ion) battery electrodes due to their faster charge transport, better conducting pathways, and good strain relaxation.[1−3] Recently, Si NW arrays[4] as well as NWs of Co_3O_4,[5,6] Fe_2O_3,[7] and SnO_2[8] in the bulk powder form have shown to retain over 75% of their maximum capacity over 10 charge−discharge cycles. However, their stability over cycling is either unknown or in some cases, capacity fading has been observed after 30−50 cycles.

Of the various metal and metal oxide materials systems, both tin (Sn) and tin oxide (SnO_2)[9,10] are interesting anode materials for Li-ion batteries because of their semiconducting properties combined with high capacity (Sn, 994 mAhg^{-1} and SnO_2, 781 mAhg^{-1})[11,12] compared to that of graphite (372 mAhg^{-1}). However, significant capacity fading with cycling is a problem specifically with metal oxide based materials due to enormous volume changes during Li alloying and dealloying leading to metal segregation and crystallographic deformation,[13] which in the case of Sn is as high as 259%.[14] So, there has been a recent interest in investigating the use of nanowire-based oxide materials to improve the capacity.

Recent studies showed that the SnO_2 nanowires and heterostructured SnO_2/In_2O_3 nanowires retain a capacity of ~700 mAhg^{-1} up to 15 cycles[8,15] but quickly fade to ~300 mAhg^{-1} after 50 cycles.[16] Similarly, SnO_2 nanorods have been shown to retain a capacity of ~400 mAhg^{-1} after 60 cycles.[17] An amorphous tin-based oxide has shown a capacity retention of ~650 mAhg^{-1} after the first cycle and significantly low fading up to 100 cycles.[10] Also, Sn/SnO_2 particle composites have been tested with capacity retention of 549 mAhg^{-1} after 40 cycles.[18] All the above studies using nanoscale tin oxide-based materials report low capacities ranging from 300 to ~620 mAhg^{-1} after 50 cycles. Therefore, it is important to develop strategies to increase the stability of nanoscale metal/metal oxide systems with high capacity retention.

Herein, we present a unique and simple generic design of hybrid structures involving metal nanoclusters covered metal oxide nanowires as stable anode materials with high reversible capacity. Although, the present study demonstrates the above concept with Sn and SnO_2 material system, it can be extended to a wide range of metal oxides, nitrides, and other semiconductors such as Si and Ge. For the present study, gram quantities of tin oxide nanowires are synthesized using a process that uses direct oxidation of tin powder in a microwave plasma. The resulting tin oxide nanowires are free of any foreign metal contamination that otherwise may hinder their electrochemical performance.

Experimental Section. SnO_2 nanowires were synthesized by reacting Sn metal powders directly in the gas phase with

* To whom correspondence should be addressed. E-mail: mahendra@louisville.edu.
[†] Department of Chemical Engineering, University of Louisville.
[‡] Department of Physics, University of Louisville.

10.1021/nl802864a CCC: $40.75
Published on Web 01/21/2009

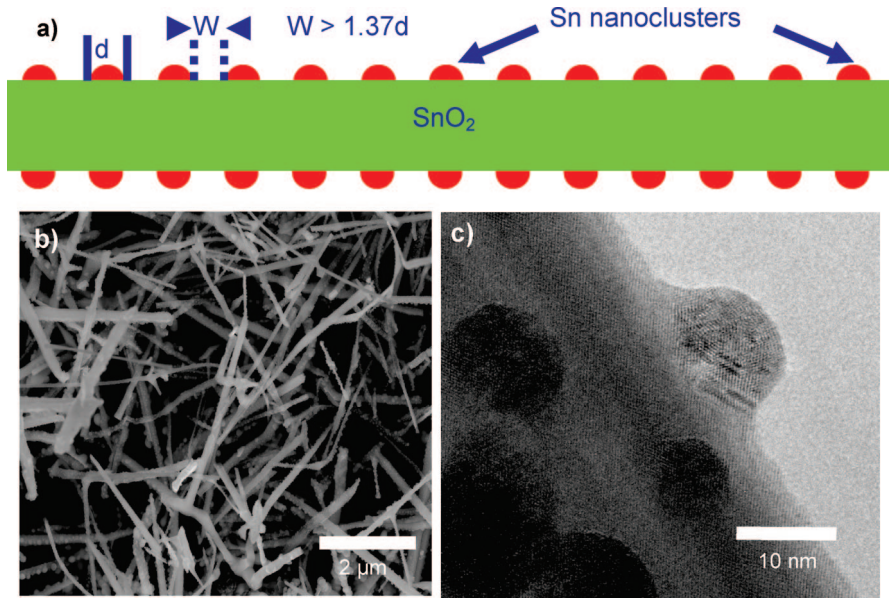

Figure 1. The concept of engineered metal nanocluster covered metal oxide nanowires. (a) Schematic showing evenly spread out Sn nanoclusters on a SnO_2 nanowire surface with spacing dependent on the droplet diameter. (b) A low-magnification SEM image showing a network of Sn-nanocluster-covered SnO_2 nanowires. (c) An HRTEM image showing well-spaced crystalline Sn nanoclusters on the nanowire periphery.

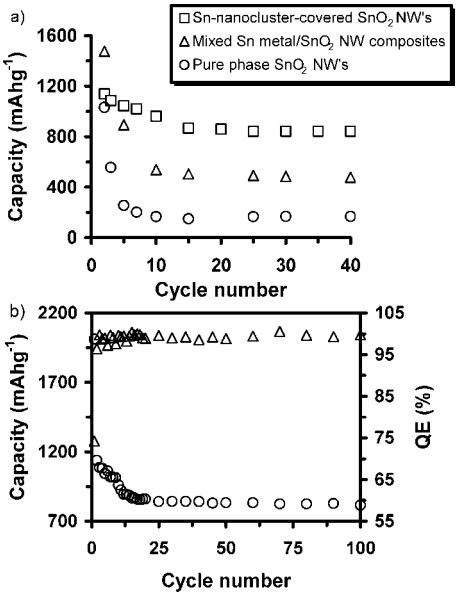

Figure 2. Electrochemical measurements of SnO_2 nanowire-based materials. (a) Cyclic performance comparison of (i) Sn-nanocluster-covered SnO_2 nanowires, (ii) SnO_2 nanowires with dispersed Sn metal, and (iii) pure SnO_2 nanowires measured between 0 to 2.2 V. Results are shown from the second cycle to the 40th cycle. (b) Capacity fading for the hybrid structures under the same conditions showing exceptional reversibility. Columbic efficiency of each cycle is also presented on the secondary *y*-axis in the right. QE = Columbic efficiency.

oxygen containing plasma without the use of a substrate in a microwave (MW) plasma jet reactor at a power of 2 kW. This process is discussed in detail elsewhere.[19] The as-synthesized SnO_2 nanowires were purified by dispersing them in 1-methoxy 2-proponal followed by gravity sedimentation. Pure SnO_2 nanowires were exposed to H_2 plasma in a microwave chemical vapor deposition reactor at a power of

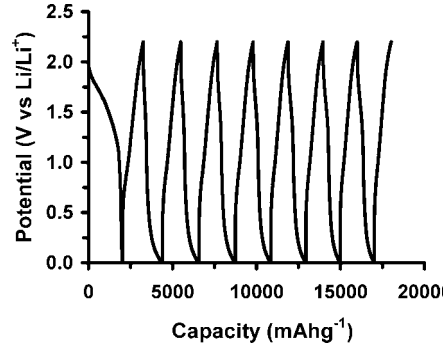

Figure 3. The voltage-capacity curves of the hybrid structures for the first eight cycles between 0 to 2.2 V performed at a rate of 100 mAg^{-1} and room temperature.

500 W for 15 min to obtain the Sn-nanocluster-covered SnO_2 nanowires. All the samples were characterized using field emission scanning electron microscopy (FE-SEM) (FEI Nova 600), X-ray diffraction (XRD) (Bruker D8 Discover), and transmission electron microscopy (TEM) (Tecnai F20 FEI TEM with a Gatan 2002 GIF system). The material for the working electrode was prepared by spreading the SnO_2 nanowire-based material uniformly on a platinum foil by applying pressure. The electrodes were made by mixing the SnO_2 nanowire-based material with carbon black and a poly(vinylidene fluoride) binder in a weight ratio of 80:10:10, respectively, in a 1-methyl-2-pyrrolidone solvent and then spreading it onto platinum foil. A three electrode cell with the SnO_2 nanowire electrode as the working electrode and lithium foil as both the reference and auxiliary (counter) electrodes was used. The electrolyte consisted of 1 M $LiPF_6$ in a 1:1 (volume) mixture of ethylene carbonate (EC) and dimethyl carbonate (DMC). The electrochemical measurements were performed using eDAQ e-corder and potentiostat in the voltage range of 0 to 2.2 V.

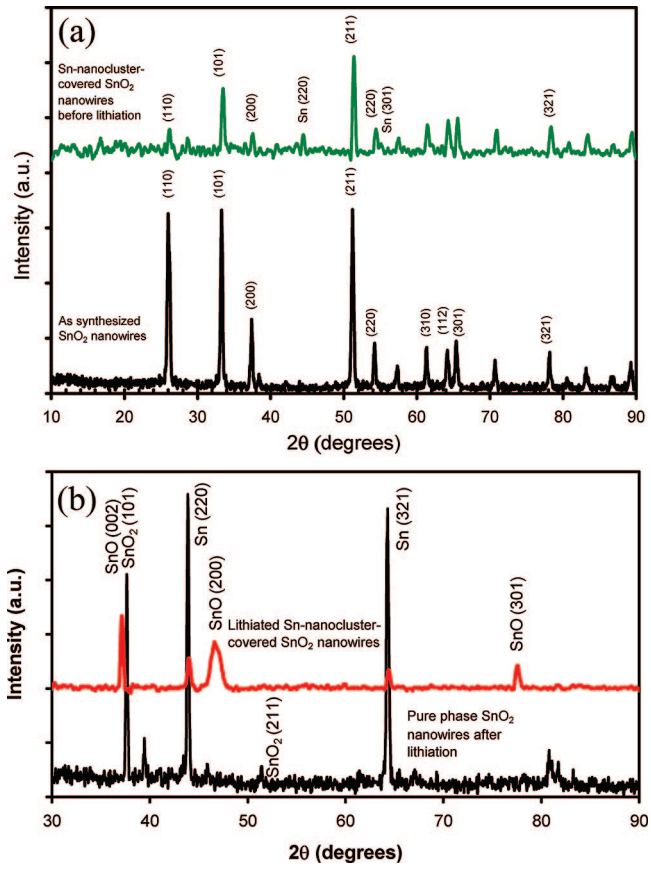

Figure 4. X-ray diffraction spectra of (a) as-synthesized SnO_2 nanowires and as-synthesized, Sn-nanocluster-covered SnO_2 nanowires and (b) lithiated pure phase SnO_2 nanowires and lithiated Sn-nanocluster-covered SnO_2 nanowires.

Results and Discussion. The design principle for the proposed hybrid structures is that the SnO_2 nanowires are covered with Sn nanoclusters with spacing ~1.4 times the diameter of each cluster as shown in Figure 1a. The spacing is necessary to accommodate the volume expansion of Sn clusters during alloying thereby preventing the Sn agglomeration. The faster electron transport through the underlying SnO_2 nanowires is expected to allow for efficient Li alloying and dealloying while the exposed Sn nanoclusters and SnO_2 nanowire surfaces serve as Li alloying sites. The SEM image in Figure 1b distinctly shows the Sn-nanocluster-covered SnO_2 nanowires with diameters ranging from 30−100 nm and a few microns long. The as-synthesized SnO_2 nanowires were reduced using H_2 plasma exposure producing nanometer-sized Sn clusters on the nanowire surfaces. The H_2 plasma exposure also reduced the nanowire diameters from 50−200 nm range to 30−100 nm range. See Figure 1c for a high resolution TEM image showing a SnO_2 nanowire covered with 15 nm sized, crystalline Sn nanoclusters evenly spaced from each other.

All materials systems are tested using anodic measurements over a potential window of 0 to 2.2 V (versus Li/Li^+). The data using pure SnO_2 nanowires showed a high initial capacity of 2400 $mAhg^{-1}$ but severe capacity degradation occurred within the next 15 cycles leading to a reversible capacity of 166 $mAhg^{-1}$ after 40 cycles as shown in Figure 2a. In comparison, Sn-nanocluster-covered SnO_2 nanowires exhibited a reversible capacity of 845 $mAhg^{-1}$ after 40 cycles as shown in Figure 2b. Other types of Sn/SnO_2 composite nanowire systems (metal Sn nanoclusters distributed in between the SnO_2 nanowire networks) showed an initial capacity of 2800 $mAhg^{-1}$ with a final reversible capacity of 490 $mAhg^{-1}$ after 40 cycles. This result is similar to that obtained in prior studies using Sn/SnO_2 composites.[18]

Figure 2b depicts the discharge specific capacity and the columbic efficiency with cycling at 100 mAg^{-1} current density, demonstrating for the first time that the mechanical stability of the material can be sustained for up to 100 cycles with an exceptional reversible capacity of 814 $mAhg^{-1}$. The hybrid structures show an initial irreversible capacity of 413 $mAhg^{-1}$, which accounts to a columbic efficiency of 74%, notably the highest reported until now in SnO_2 systems. See the secondary axis in Figure 2b. The columbic efficiency in the subsequent cycles is shown to be over 98%. The capacity fading at a rate of ~1.3% for the initial 15 cycles and ~0.8% after the 15th cycle is considerably lower than that reported for other nanoscale SnO_2 material systems.[8,16] The reasons for enhanced capacity retention and Coulombic efficiency could be attributed to their high surface area to volume ratio which increases the net amount of Li alloying and dealloying. Figure 3 shows the initial charge and discharge curves of the hybrid SnO_2 structures in a potential window of 0 to 2.2 V. High discharge capacity of 2013 $mAhg^{-1}$ in the first cycle is attributed to the fact that Li intercalates into SnO_2 during the first cycle followed by the subsequent alloying of Li with Sn forming a Li_xSn alloy, which corresponds to the plateau observed below 0.5 V in the charge−discharge curves. For pure phase SnO_2 nanowires, rapid capacity degradation is observed with cycling and capacity retention of 166 $mAhg^{-1}$ is obtained after 40 cycles. The XRD and SEM characterization of the material after cycling showed that the SnO_2 NWs reduce completely to Sn while destroying the nanowire morphology. These observations about severe degradation of nanowire morphology and reduction in the capacity are consistent with prior studies involving SnO_2 and other metal oxide nanowires.[8,15,16] In some cases, the as-synthesized SnO_2 nanowire samples have exhibited capacity retention over a range of values (166−300 $mAhg^{-1}$), which is possibly due to the presence of some excess Sn metal on nanowire surfaces similar to our hybrid nanowire systems. Complete reduction of the SnO_2 nanowires at various microwave powers yielded Sn crystals of varying diameters rather than Sn nanowires. SEM image of the completely reduced system is shown in the Supporting Information. The performance of Sn thin films as anodes has been studied before[20] and performs similarly to that of pure phase SnO_2 system, that is, the capacity fades quickly to about 200 $mAhg^{-1}$ in 20 cycles.

The stability of the Sn-nanocluster-covered SnO_2 nanowires could possibly be explained with the following Li alloying mechanism:[21]

$$SnO_2 + 2Li^+ + 2e^- \rightarrow SnO + Li_2O \quad (1)$$

$$SnO + 2Li^+ + 2e^- \rightarrow Sn + Li_2O \quad (2)$$

$$Sn + xLi^+ + xe^- \leftrightarrow Li_xSn\ (0 \le x \le 4.4) \quad (3)$$

The reaction of SnO_2 with Li ions, electrolyte decomposition, and solid electrolyte interface formation are believed to be the reasons for large irreversible capacity during the first cycle. In the case of pure SnO_2 materials including nanowires, the reduction of SnO_2 to Sn takes place in the first cycle. Repeated cycling induces enormous volume changes in Sn that tends to expand and coalesce with the nearby Sn atoms, leading to large agglomerates, thus reducing the available surface area for the Li-ion storage capacity of the material and eventually destroys the pure oxide nanowire structure.

In the case of our hybrid structures involving Sn-nanocluster-covered SnO_2 nanowires, the spacing between clusters was adequate enough to accommodate the volume changes induced by the lithiation process, preventing agglomeration thus explaining high capacity even after hundred charge−discharge cycles. In addition, the underlying nanowires must retain both morphology and conductivity for the observed stability with cycling. So, the XRD spectra were obtained for both pure phase and Sn-nanocluster-covered SnO_2 nanowire samples after they were subjected to several charge−discharge cycles. Figure 4a depicts the XRD spectra of as-synthesized rutile phase SnO_2 nanowires and Sn-nanocluster-covered SnO_2 nanowires. Figure 4b shows the XRD spectra of both pure phase and Sn-nanocluster-covered SnO_2 nanowires after 25 and 100 charge and discharge cycles, respectively. After lithiation, the majority of the SnO_2 nanowires get completely converted into Sn phase in the case of pure SnO_2 nanowire samples along with unreacted SnO_2 phases. In comparison, the Sn-nanocluster-covered SnO_2 nanowires after hundred charge−discharge cycles show the presence of SnO phase in addition to Sn phases. The observed, small peak shifts with both SnO (301) and SnO (002) peaks toward the lower diffraction angle indicate that the observed SnO phase might be a lithiated SnO phase. The observed capacity retention can be attributed to the presence of Sn as well as SnO phase. The SnO phase is formed as a result of the reversibility of eq 3 in which the nanoscale Sn domains can decompose the Li_2O, which is otherwise irreversible. This reversibility gives rise to the formation of SnO nanodomains from Sn-nanosized particles during the delithiation process. Such nanodomains are clearly seen to be present in an amorphous matrix within the nanowires after they were subjected to 100 charge−discharge cycles. See the high-resolution TEM (HRTEM) image in Figure 5b. The reversibility of the metal particles to metal oxides by the decomposition of Li_2O in nanosized domains was shown to be feasible in other reports.[1,6]

The SEM image in Figure 5a distinctly shows unblemished hybrid nanowires after 100 charge−discharge cycles. However, the image shows the enlarged Sn nanoclusters on the nanowire periphery that is due to the volume expansion of Sn as well as the Sn segregation from the interior of the nanowire. The proposed reversibility with the Sn nanocluster-covered SnO_2 nanowires is schematically illustrated in Figure

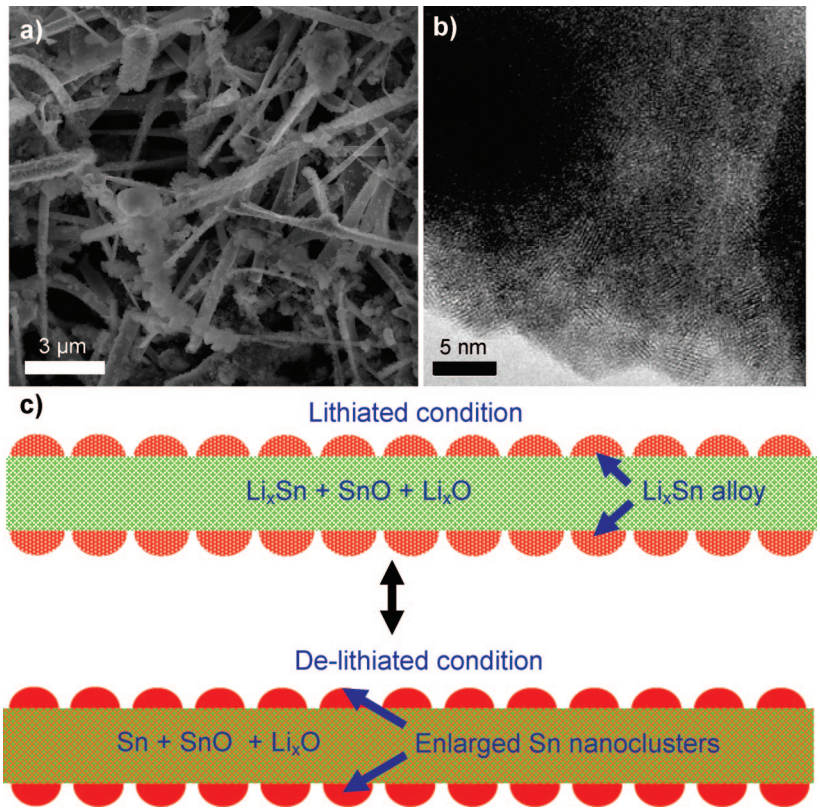

Figure 5. Characterization of hybrid structures after 100 cycles of charge and discharge. (a) SEM image of hybrid nanowires. (b) HRTEM image of the Sn nanocluster-covered SnO_2 nanowires. (c) A schematic illustrating the reversible Li alloying and dealloying steps in the Sn-nanocluster-covered-SnO_2 nanowires.

5c. As shown in the schematic, the nanowire is composed of SnO and Li_xO in which SnO promotes the electronic conductivity while the Li_xO phase promotes the Li-ion migration during Li alloying and dealloying stages as well as prevents further Sn agglomeration inside the nanowire.[18] Hence, the nanowire morphology is retained after several cycles avoiding major structural changes. The SnO phase could also arise due to the slightly reversible nature of the reaction in eq 2 during the dealloying process, that is, the faster kinetics for SnO formation compared to SnO_2.[22,23]

Conclusions. In summary, a new class of hybrid structures involving SnO_2 nanowires decorated with well-separated Sn nanoclusters exhibit a reversible storage capacity greater than 800 $mAhg^{-1}$ over 100 cycles. These hybrid structures with improved stable capacity better relieve the stresses associated with volume changes compared to the pure phase SnO_2 nanowires. The capacity fading after the first few cycles is the lowest at less than 1% per cycle. Post-lithiated samples show the intact hybrid structure after 100 cycles. The proposed new concept could be applied to other nanoscale metal oxide, nitride systems including Co_3O_4 ($\sim$900 $mAhg^{-1}$)[1] and other material systems, such as Si,[4] leading to stable and high capacity Li-ion batteries and could lead to major advancements in portable power applications.

Acknowledgment. The authors gratefully acknowledge the financial support from the U.S. Department of Energy (DE-FG02-05ER64071 and DE-FG02-07ER46375).

Supporting Information Available: The details of the pure phase SnO_2 nanowire electrode performance including the electrochemical testing (capacity curves), postlithiation characterization (SEM and XRD) are included. The XRD peak analysis of the postlithiated Sn-nanocluster-covered SnO_2 electrode is also presented. This material is available free of charge via the Internet at http://pubs.acs.org.

References

(1) Poizot, P.; Laruelle, S.; Grugeon, S.; Dupont, L.; Tarascon, J.-M. *Nature* **2000**, *407*, 496.
(2) Aricó, A. S.; Bruce, P.; Scrosati, B.; Tarascon, J.−M.; Schalkwijk, W. V. *Nat. Mater.* **2005**, *4*, 366.
(3) Taberna, P. L.; Mitra, S.; Poizot, P.; Simon, P.; Tarascon, J.-M. *Nat. Mater.* **2006**, *5*, 567.
(4) Chan, C. K.; Peng, H.; Liu, G.; McIlwrath, K.; Zhang, X. F.; Huggins, R. A.; Cui, Y. *Nat. Nanotechnol.* **2008**, *3*, 31.
(5) Nam, K. T.; Kim, D.−W.; Yoo, P. J.; Chiang, C.-Y.; Meethong, N.; Hammond, P. T.; Chiang, Y.-M.; Belcher, A. M. *Science* **2006**, *312*, 885.
(6) Li, Y.; Tan, B.; Wu, Y. *Nano Lett.* **2008**, *8*, 265.
(7) Chen, J.; Xu, L.; Li, W.; Gou, X. *Adv. Mater.* **2005**, *17*, 582.
(8) Ying, Z.; Wan, Q.; Cao, H.; Song, Z. T.; Feng, S. L. *Appl. Phys. Lett.* **2005**, *87*, 113108.
(9) Idota, Y.; Kubota, T.; Matsufuji, A.; Maekawa, Y.; Miyasaka, T. *Science* **1997**, *276*, 1395.
(10) Kim, E.; Son, D.; Kim, T.−G.; Cho, J.; Park, B.; Ryu, K.-S.; Chang, S.-H. *Angew. Chem., Int. Ed.* **2004**, *43*, 5987.
(11) Winter, M.; Besenhard, J. O. *Electrochim. Acta* **1999**, *45*, 31.
(12) Derrien, G.; Hassoun, J.; Panero, S.; Scrosati, B. *Adv. Mater.* **2007**, *19*, 2336.
(13) Wachtler, M.; Winter, M.; Besenhard, J. O. *J. Power Sources* **2002**, *105*, 151.
(14) Boukamp, B. A.; Lesh, G. C.; Huggins, R. A. *J. Electrochem. Soc.* **1981**, *128*, 725.
(15) Kim, D.-W.; Hwang, I.-S.; Kwon, S. J.; Kang, H.-Y.; Park, K.-S.; Choi, Y.-J.; Choi, K.-J.; Park, J.-G. *Nano Lett.* **2007**, *7*, 3041.
(16) Park, M.-S.; Wang, G.-X.; Kang, Y.-M.; Wexler, D.; Dou, S.-X.; Liu, H.-K. *Angew. Chem., Int. Ed.* **2007**, *46*, 750.
(17) Wang, Y.; Lee, J. Y. *J. Phys. Chem. B* **2004**, *108*, 17832.
(18) Sivashanmugam, A.; Prem Kumar, T.; Renganathan, N. G.; Gopukumar, S.; Wohlfahrt-Mehrens, M.; Garche, J. *J. Power Sources* **2005**, *144*, 197.
(19) Kumar, V.; Kim, J. H.; Pendyala, C.; Chernomordik, B.; Sunkara, M. K. *J. Phys. Chem. C* **2008**, *112*, 17750.
(20) Morimoto, H.; Tobishima, S.; Negishi, H. *J. Power Sources* **2005**, *146*, 469.
(21) Li, N.; Martin, C. R. *J. Electrochem. Soc.* **2001**, *148*, A164.
(22) Sandu, I.; Brousse, T.; Schleich, D. M.; Danot, M. *J. Solid State Chem.* **2006**, *179*, 476.
(23) Courtney, I. A.; Dunlap, R. A.; Dahn, J. R. *Electrochim. Acta* **1999**, *45*, 51.

NL802864A